Hindawi Publishing Corporation
Journal of Nanomaterials
Volume 2015, Article ID 745217, 10 pages
http://dx.doi.org/10.1155/2015/745217

Research Article

Development of Castor Oil Based Poly(urethane-esteramide)/TiO_2 Nanocomposites as Anticorrosive and Antimicrobial Coatings

Mohammed Rafi Shaik,[1] Manawwer Alam,[2] and Naser M. Alandis[1]

[1]*Department of Chemistry, College of Science, King Saud University, P.O. Box 2455, Riyadh 11451, Saudi Arabia*
[2]*Research Center, College of Science, King Saud University, P.O. Box 2455, Riyadh 11451, Saudi Arabia*

Correspondence should be addressed to Manawwer Alam; malamiitd@gmail.com

Received 2 September 2014; Accepted 15 December 2014

Academic Editor: Antonios Kelarakis

Castor oil based polyesteramide (CPEA) resin has been successfully synthesized by the condensation polymerization of N-N-bis (2-hydroxyethyl) castor oil fatty amide (HECA) with terephthalic acid and further modified with different percentages of 7, 9, 11, and 13 wt.% of toluene-2,4-diisocyanate (TDI) to obtain poly(urethane-esteramide) (UCPEA), via addition polymerization. TiO_2 (0.1, 0.2, 0.3, 0.4, and 0.5 wt%) nanoparticles were dispersed in UCPEA resin. The structural elucidation of HECA, CPEA, and UCPEA has been carried out using FT-IR, ^{1}H-NMR, and ^{13}C-NMR spectroscopic techniques while physicochemical and physicomechanical properties were investigated by standard methods. Thermal stability and molecular weight of UCPEA have been assessed by thermogravimetric analysis (TGA) and gel permeation chromatography (GPC), respectively. Furthermore, the corrosion behavior of UCPEA coatings on mild steel has been investigated by potentiodynamic polarization measurements in different corrosive environments (3.5 wt% HCl, 5 wt% NaCl, 3.5 wt% NaOH, and tap water) at room temperature and surface analysis by scanning electron microscope (SEM) and energy dispersive X-ray (EDX). The antibacterial activities of the UCPEA were tested against bacteria and fungi by agar disc diffusion method. The results of this study have revealed that UCPEA nanocomposite coatings exhibit good physicomechanical, anticorrosion and antimicrobial properties, which can be safely used up to 200°C.

1. Introduction

Vegetable oils have recently gained a lot of interests owing to the fact that they are renewable resources and possess high environmental benefits. Vegetable oils such as castor oil, linseed oil, soybean oil, rapeseed, olive, cottonseed, *Jatropha*, *Pongamia glabra*, rubber seed, and *Jojoba* oil are used in chemical industries for the manufacturing of coatings, surfactants, soaps cosmetic products, lubricants, and paints [1–3]. Castor oil is viscous, pale yellow, and nondrying oil with a bland taste and one of the cheapest renewable resources for production of ecofriendly resins. Castor oil (*Ricinus communis*) is obtained from seeds of plant, which belong to the family Euphorbiaceae. Castor oil consisting of triglycerides containing 90% ricinoleic acid (12-hydroxy-9-octadecenoic acid), and 10% non-functional acid residues [4]. Castor oil is also distinguished from other vegetable oils by its high specific gravity and hydroxyl value. Therefore, a lot of research work is being carried out towards the production of vegetable oil based polymeric materials possessing good physical and chemical properties [5–7]. Moreover, castor oil based polymers are biodegradable, cheap, easy to modify, and easily available in large quantities [8].

Vegetable oils based biopolymers such as alkyd [9], polyurethane [10], epoxy [11], polyesteramide [12], and polyetheramide [5, 13] are used in the area of paint and coatings. These polymers are biodegradable, less volatile content, environmental friendly, nontoxic, and inexpensive materials. Therefore several biopolymers have been prepared using various vegetable oil. Previously, castor oil is mainly used for synthesis of polyesteramide, interpenetrating polymer network (IPN), polyurethane, epoxy, and blending with commercial

polymethylmethacrylate, polystyrene, polyvinyl alcohol, and so forth [14].

The antimicrobial coating property is undoubtedly priority for investigators of material science in the world. The nanoparticles (NPs) in surface coatings can be used to improve gloss, impact resistance, scratch hardness, pencil hardness, and antimicrobial properties [15]. NPs dimensions of less than 100 nm are adequate to reinforce polymer matrix without disturbing the transparency and other properties of the coatings. In the field of surface coatings frequently used nanoparticles are TiO_2, Ag_2O, Al_2O_3, and others [16–21]. Polymers containing TiO_2 (NPs) had attracted significant attention due to their execute biocidal properties with their less volatile nature [22–27]. Literature survey reveals that castor oil based poly(urethane-esteramide)/TiO_2 nanocomposite coatings are not reported yet.

Herein, we report the synthesis of castor oil polyesteramide (CPEA) using terephthalic acid and further modified by toluene-2,4-diisocyanate (TDI) to obtained poly(urethane-esteramide) (UCPEA) with TiO_2 NPs to form poly(urethane-esteramide) nanocomposite. CPEA and UCPEA were characterized using FT-IR, ^{1}H-NMR, and ^{13}C-NMR spectroscopic techniques. The incorporation of ester and urethane moieties in polymer chain improved its physicomechanical and chemical resistance properties.

2. Experimental

2.1. Materials. Castor oil (Avonchem, UK), sodium, methanol (Sigma Aldrich), diethanolamine (Winlab, UK), terephthalic acid (Prolabo laboratories, Rhone), titanium isopropoxide (Aldrich Chemical, UK), isopropanol (Merck, India), xylene, butanone (Winlab, UK), and toluene-2,4-diisocyanate (Acros Organics, USA) were of analytical grade.

2.2. Synthesis

2.2.1. N, N-Bis (2-hydroxyethyl) Castor Oil Fatty Amide (HECA). Diethanolamine (50 g) and sodium methoxide (0.26 g) were mixed in round flask fitted with a stirrer, dropping funnel, and thermometer. Castor oil (60 g) was added dropwise for a period of 0.5 h, at a temperature of 120 ± 5°C. The reaction progress was monitored by thin layer chromatography (TLC). After completion the reaction mixture was washed with diethyl ether and 15% aqueous NaCl solution and then dried using anhydrous sodium sulphate. The diethyl ether was removed by rotatory vacuum evaporator and a light brown colour of HECA obtained [5, 26, 27].

2.2.2. Castor Oil Polyesteramide (CPEA). 0.10 mol of HECA and 0.07 mol of terephthalic acid were dissolved in 100 mL of xylene kept in three-neck round bottom flask equipped with dean stark trap, N_2 inlet, and thermometer, and stirrer has been used. The reaction mixture was heated up to 250°C and progress of reaction was monitored by TLC and acid value (8–10). On completion of reaction, solvent was evaporated in vacuum evaporator to obtain CPEA.

2.2.3. Castor Oil Poly(urethane-esteramide) (UCPEA). CPEA was mixed with TDI in different proportions (7, 9, 11, and 13 wt%), in xylene with continuous stirring in four-neck flask was used under N_2 atmosphere at 120°C. The reaction was monitored by TLC as well as hydroxyl value determination at regular intervals of time.

2.2.4. Poly(urethane-esteramide)/TiO_2 Nanocomposites. TiO_2 NPs were added in prepared UCPEA resin with various concentrations, namely, 0.1 wt%, 0.2 wt%, 0.3 wt%, 0.4 wt%, and 0.5 wt%. The dispersion was carried out mechanically using a magnetic stirrer with high speed of 200 rpm for 30 min at room temperature. 0.4 wt% NPs showed best dispersion in polymer matrix and also good physicomechanical properties. 0.4 wt% NPs were used for all synthesized resins like UCPEA-7, UCPEA-9, UCPEA-11, and UCPEA-13.

2.2.5. TiO_2 Nanoparticles. The precursor solution was a mixture of 5 mL titanium isopropoxide, 15 mL isopropanol, and 250 mL solution of distilled water used as hydrolysis catalyst. The desired pH = 2 value of solution was adjusted by adding nitric acid or ammonium hydroxide. The gel preparation process started when both solutions were mixed together under vigorous stirring. Hydrolysis of titanium isopropoxide resulted into a turbid solution, which was heated up to 60–70°C for 18–20 hours. The resultant suspension was white-blue in colour, which was obtained as precipitates were formed. The precipitates were washed with ethanol and dried for 4 hours at 100°C and finally annealed at 800°C for 2 hours [28].

2.3. Characterization. HECA, CPEA, and UCPEA resins have been characterized using spectroscopic techniques such as FT-IR, ^{1}H-NMR, and ^{13}C-NMR. FT-IR spectra of these polymers have been carried out on Prestige-21, FTIR-8400S, Shimadzu Corporation, Kyoto, Japan (using NaCl cell). ^{1}H-NMR and ^{13}C-NMR spectra have been recorded on a Jeol DPX 400 MHz using deuterated chloroform ($CDCl_3$) as solvent and tetramethylsilane (TMS) as an internal standard. Thermal analysis was carried out by thermogravimetric analysis (TGA) that was measured with TGA/DSC1, Mettler Toledo AG, Analytical CH-8603 Schwerzenbach, Switzerland, in nitrogen atmosphere at a heating rate of 10°C/minute. The physicochemical properties such as iodine value (ASTM D1959-97), hydroxyl value (ASTM D1957-86), acid value (ASTM D55-61), and refractive index were determined by standard laboratory method. Molecular weight distribution curve and relative values of number average (Mw) and weight average (Mn) molecular weight of UCPEA have been determined using GPC (HT-GPC Module 350A, Viscotek, Houston, TX 77060, USA; GPC equipped with CLM6210 HT-GPC column) with polystyrene standard at 30°C and carrier solvent tetrahydrofuron (THF) with flow rate 1.0 mL/min. Molecular weight measured for UCPEA was 41,217 (Mn), 62400 (Mw) and polydispersity index 1.513.

The prepared titanium dioxide nanoparticles were investigated for their size by using TEM (JEM-2100F, Field emission electron microscope, JEOL, Japan). The analysis was carried out by accelerating voltage in the range of 20–200 kV

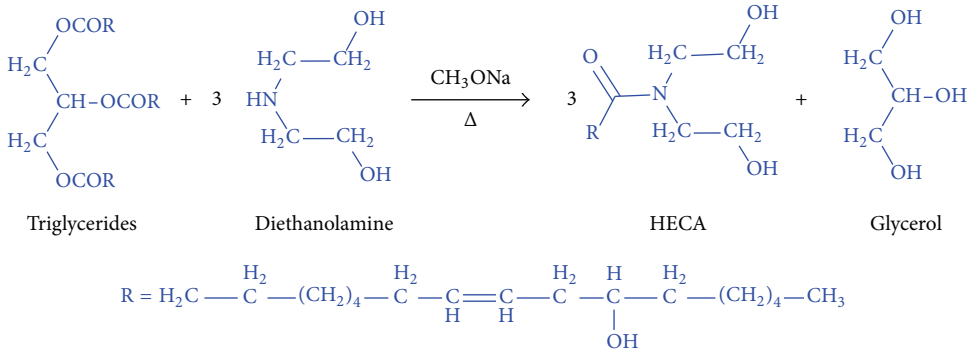

Scheme 1: Synthesis of HECA.

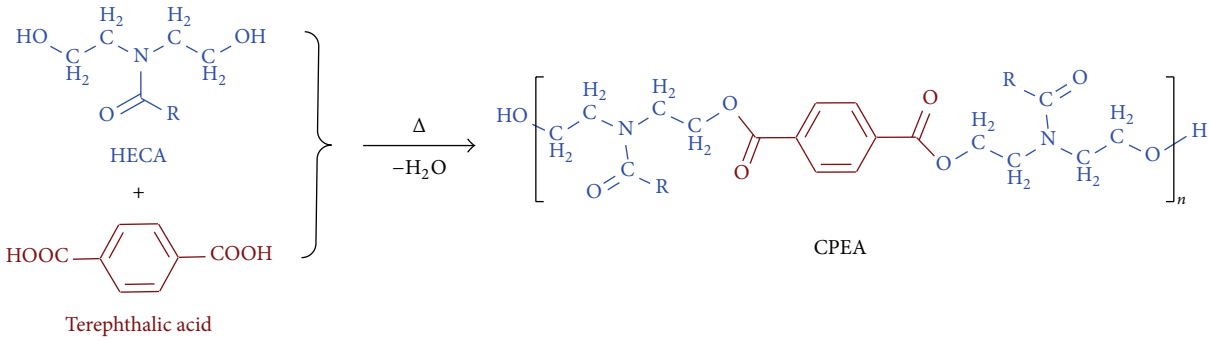

Scheme 2: Synthesis of CPEA.

with 2.4 Å resolution by dispersion TiO_2 in ethanol with ultrasonic wave for one hour. After sonication sample was deposited on Cu grid and observed at high magnification. The size of TiO_2 nanoparticles was observed in range of 20–50 nm (Figure 10).

The antibacterial and antifungal activity of UCPEA-13 was investigated by agar disc diffusion method. The microorganisms used in this study were three bacteria, *Staphylococcus aureus*, *Escherichia coli*, and *Bacillus pasteurii*, and three fungal strains, *Fusarium solani*, *Penicillium notatum*, and *Aspergillus niger*. The culture was prepared for antibacterial studies, nutrient agar [27]. 1 wt% solution of UCPEA-13 in xylene was used for growth studies of bacteria at 27°C (incubator temperature). Potato dextrose broth was used for cultivation of fungi. Antifungal activity of UCPEA-13 was tested against pathogenic fungi with concentrations of 100 μg/disc for each and xylene for control. The activity was determined after 72 h of incubation at 32°C.

2.4. Preparation of Coatings. 40 wt% solutions of UCPEA resins were applied by dip technique on commercial available mild steel strips. The UCPEA coatings on mild steel strips were tested for impact resistance (IS: 101 part 5/sec. 3, 1988), scratch hardness (BS 3900), and bend test (1/8 inch conical mandrel, ASTM-D3281-84) that were performed on all compositions of UCPEA coatings. Moreover, specular gloss of coatings was determined at 45°C using Gloss-meter (Model RSPT 20; digital instrument, Santa Barba, CA, USA). Coating thickness is measured using Elcometer (Model 456; Elcometer instrument, Manchester, UK). Corrosion resistance studies of UCPEA coated mild steel were also performed using Gill AC (ACM Instruments, UK). Geometric area of 1 cm^2 each for coated steel was exposed to different corrosive media 3.5 wt% NaOH, 3.5 wt% HCl, 5 wt% NaCl, and tap water. Corrosion current (I_{corr}) and corrosion potential (E_{corr}) were measured using potentiodynamic polarization. The corrosion inhibition efficiency (IE) was calculated according to a reported paper [29].

3. Results and Discussion

Schemes 1, 2, and 3 show the synthesis of HECA, CPEA, and UCPEA, respectively. HECA was obtained by the reaction of diethanolamine with castor oil. HECA was reacted with terephthalic acid to form CPEA and further treated with TDI with addition of TiO_2 nanoparticles to obtain UCPEA nanocomposite. The structural features of HECA, CPEA, and UCPEA have been confirmed by FT-IR, ^{1}H-NMR, and ^{13}C-NMR spectral analysis.

3.1. Spectral Analysis

3.1.1. FT-IR. FT-IR spectra of HECA, CPEA, and UCPEA are shown in Figure 1. HECA spectra show a characteristic broadband of hydroxyl group appearing at 3383 cm^{-1}, $-CH_2-$ symmetrical and asymmetric stretching occurs at 2926 and

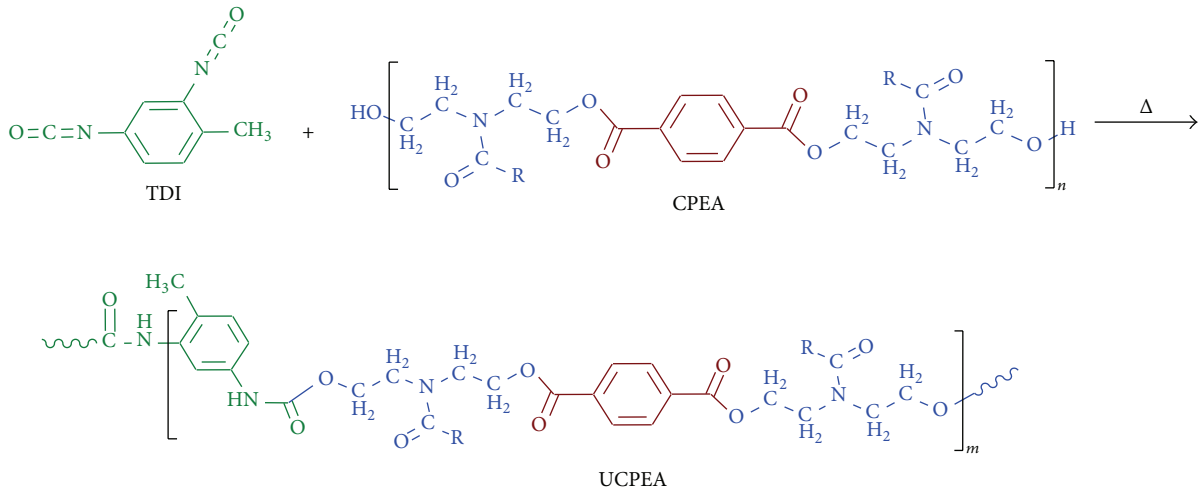

Scheme 3: Synthesis of UCPEA.

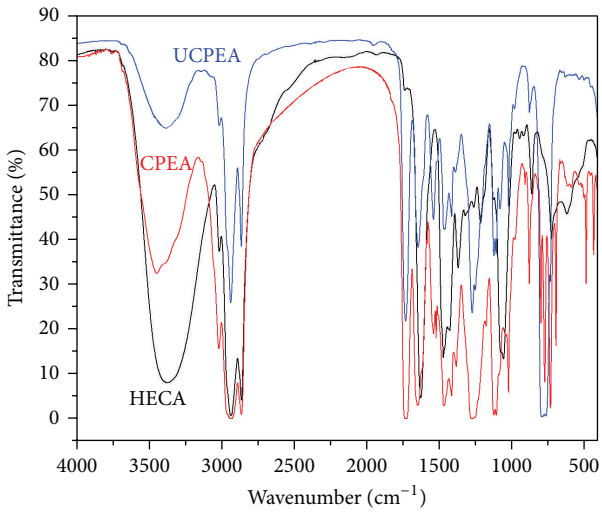

Figure 1: FT-IR spectra of HECA, CPEA, and UCPEA.

2852 cm^{-1}. The amide carbonyl bands and C–N stretching bands are found at 1617 cm^{-1}, 1459 cm^{-1}. In spectra of CPEA, the above-mentioned absorption bands are observed along with some additional bands. The band at 3393 cm^{-1} is for hydroxyl group but in this case of CPEA intensity decreases when compared to HECA and additional band at 1729 cm^{-1} appears belonging to carbonyl ester group. 1534, 775, 724 cm^{-1} bands belong to aromatic ring of terephthalic acid. The spectrum of UCPEA shows some additional bands also observed at 1721 cm^{-1} representing urethane linkages, bands at 3010, 1530, 1409, and 775 cm^{-1} for –CH=CH–, aromatic ring of terephthalic acid and residual hydroxyl group at 3393 cm^{-1}.

3.1.2. ^{1}H-NMR. ^{1}H-NMR spectra of HECA: it can be inferred that characteristic peak of terminal C**H**$_3$ appears at δ = 0.83 ppm. The peaks at δ = 4.8 ppm and δ = 5.29 ppm indicate alcoholic protons adjacent to –CH$_2$ and –C**H**=C**H**– group, respectively. The C**H**$_2$ proton attached to the amide nitrogen was obtained at δ = 3.71 ppm and δ = 3.62 ppm peak is due to –C**H** proton adjacent to alcoholic group. ^{1}H-NMR of CPEA (Figure 2(a)) shows the characteristic peaks at δ = 4.15–4.23 ppm corresponding to –C**H**$_2$– linked with ester group confirming the formation of ester in reaction of HECA with terephthalic acid. The –C**H**$_3$ and C**H**$_2$ for terminal and internal fatty amide chains were apparently observed at δ = 0.83 and δ = 1.22–1.40 ppm, respectively. While –C**H**$_2$– linked with olefinic double bond at δ = 2.15–2.34 ppm, characteristic peaks for –C**H**$_2$– attached to amide nitrogen and that of amide carbonyl are both present at δ = 3.56–3.77 ppm and δ = 2.4–2.29 ppm, respectively. Peaks at δ = 3.50–3.59 and δ = 5.29–5.35 ppm are all characteristic peaks for C**H**$_2$ attached to hydroxyl and olefinic protons, respectively. δ = 7.23–7.25 shows aromatic ring. These peaks confirm the reaction between HECA with terephthalic acid. ^{1}H-NMR spectra of UCPEA (Figure 2(b)) confirm structure as shown in Scheme 3 with characteristic peaks of –C**H**$_2$ attached to urethane linkage at δ = 2.34–2.41 ppm, –C**H**$_3$ of TDI at δ = 2.26 ppm while aromatic protons appeared at δ = 7.26–7.29 ppm. The observed peak for –N**H** of urethane is at δ = 7.8 ppm.

3.1.3. ^{13}C-NMR. ^{13}C-NMR spectra of HECA: presence of signals at δ = 14.17 ppm (terminal **C**H$_3$), δ = 22.3 ppm (COCH$_2$–**C**H$_2$–), δ = 60.61–60.95 (–**C**H$_2$OH), δ = 52.22 ppm (–**C**H$_2$N–), δ = 127.92–130.22 ppm (–**C**H=**C**H–), δ = 175.58 ppm (**C**=O, amide). In CPEA spectra of Figure 3(a) show the characteristic peaks at δ = 14.17 ppm (terminal **C**H$_3$), δ = 22.68–31.90 ppm of (–**C**H$_2$–), and other peaks at δ = 62.19 ppm show (–**C**H$_2$–) attached to nitrogen: δ = 125.44–129.79 (aromatic ring); δ = 176.10, 166.20 ppm (**C**=O, amide, ester). In UCPEA spectra (Figure 3(b)) show appearance of –**C**H$_3$ peaks for TDI at δ = 22.65 ppm δ = 125.48 ppm showing aromatic ring. δ = 165.21 ppm appears to be (**C**=O, urethane).

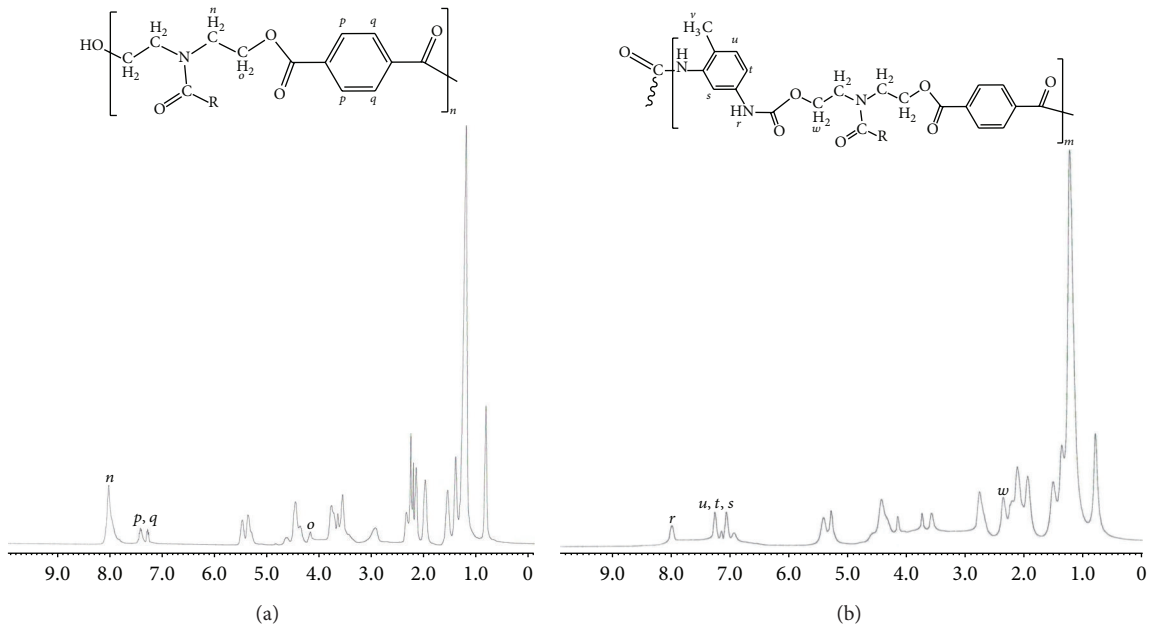

Figure 2: (a) ^{1}H-NMR spectra of CPEA. (b) ^{1}H-NMR spectra of UCPEA.

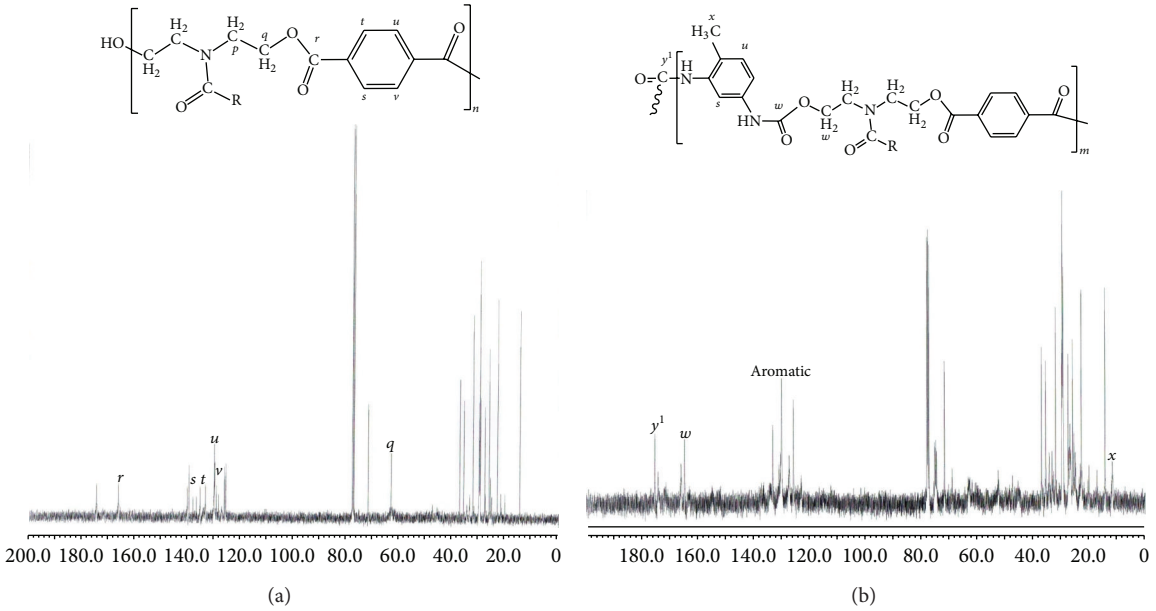

Figure 3: (a) ^{13}C-NMR spectra of CPEA. (b) ^{13}C-NMR spectra of UCPEA.

3.2. Physicochemical Characterization. Physicochemical characteristics as shown in Table 1 indicate decrease in hydroxyl and iodine values from HECA, CPEA, UCPEA-7, UCPEA-9, UCPEA-11, and UCPEA-13. This sudden decrease in hydroxyl value from HECA to CPEA might have resulted from the reaction of hydroxyl groups of HECA with terephthalic acid that formed CPEA. Moreover, the decrease in iodine value could be associated to increase in molar mass of CPEA as compared to HECA. Furthermore, a small decrease in hydroxyl value has been observed with gradual loading of TDI. This might be the effect of reaction on hydroxyl groups of CPEA with –NCO of TDI which resulted in UCPEA. This reaction further caused increase in molar mass of polymer and further decrease in iodine values. The increase in refractive index from HECA, CPEA, UCPEA-7, UCPEA-9, UCPEA-11, and UCPEA-13 could be associated with increase in molar mass of system in that sequence.

3.3. Coating Properties. The poly(urethane-esteramide) coatings containing TiO_2 nanoparticles were applied on mild

Table 1: Physicochemical and physicomechanical characterization of resins.

Characteristics	Castor oil	HECA	CPEA	UCPEA-7	UCPEA-9	UCPEA-11	UCPEA-13
Acid value	0.8	1.7	8.0	—	—	—	—
Hydroxyl value	149	8.12	6.15	4.92	4.5	3.4	3.2
Iodine value	83	48	30.2	20.01	19.1	18.2	17.5
Refractive index	1.606	1.611	1.601	1.603	1.605	1.607	1.611
Impact resistance (lb/in)	—	—	—	150	150	150	150
Gloss at 45°	—	—	—	84	88	91	93
Thickness (micron)	—	—	—	140	162	165	163
Pencil hardness	—	—	—	2H	3H	4H	4H
Scratch Hardness (kg)	—	—	—	1.5	1.6	1.7	1.6
Bend test (1/8 inch)	—	—	—	Passes	Passes	Passes	Passes

Table 2: Corrosion parameter for coated and uncoated MS in different corrosive environments.

Sample code	Medium	E_{corr} (mV)	I_{corr} (mA/cm^2)	Corrosion rate (mm/yr)	βA	βC	Inhibition efficiency (%)
Mild steel	3.5 wt% HCl	−483.06	2.5857	27.65	93.13	137.71	—
UCPEA-7	3.5 wt% HCl	−515.35	4.959×10^{-4}	6.810×10^{-2}	445.41	431.92	99.98
UCPEA-9	3.5 wt% HCl	−249.58	9.750×10^{-5}	1.130×10^{-3}	462.99	154.16	99.77
UCPEA-11	3.5 wt% HCl	−480.31	4.045×10^{-6}	4.688×10^{-5}	431.04	860.86	99.99
UCPEA-13	3.5 wt% HCl	419.22	1.129×10^{-7}	1.309×10^{-6}	391.37	247.72	99.99
Mild steel	5.0 wt% NaCl	−760.85	4.445×10^{-1}	5.1627	102.06	138.85	—
UCPEA-7	5.0 wt% NaCl	−561.09	2.251×10^{-3}	2.609×10^{-2}	372.72	209.89	99.38
UCPEA-9	5.0 wt% NaCl	−573.97	1.746×10^{-4}	2.024×10^{-3}	280.21	321.94	99.96
UCPEA-11	5.0 wt% NaCl	−449.39	1.215×10^{-3}	1.408×10^{-2}	179.77	183.25	99.72
UCPEA-13	5.0 wt% NaCl	−107.86	8.271×10^{-7}	9.587×10^{-6}	318.32	253.65	99.99
Mild steel	Tap water	−474.96	3.366×10^{-2}	3.901×10^{-1}	111.62	526.04	—
UCPEA-7	Tap water	−661.63	4.281×10^{-4}	4.962×10^{-3}	353.43	277.28	98.72
UCPEA-9	Tap water	−577.37	3.190×10^{-4}	3.697×10^{-3}	484.94	157.34	99.05
UCPEA-11	Tap water	−659.04	9.760×10^{-5}	1.113×10^{-4}	288.57	311.79	99.71
UCPEA-13	Tap water	−515.14	8.654×10^{-5}	1.003×10^{-3}	307.27	224.87	99.74
Mild steel	3.5 wt% NaOH	−455.70	1.787×10^{-3}	2.071×10^{-2}	272.36	246.63	—
UCPEA-7	3.5 wt% NaOH	−458.32	9.850×10^{-5}	1.141×10^{-3}	596.21	192.97	94.09
UCPEA-9	3.5 wt% NaOH	−445.21	1.180×10^{-3}	1.368×10^{-2}	334.64	165.38	33.96
UCPEA-11	3.5 wt% NaOH	−426.85	1.180×10^{-3}	1.368×10^{-2}	336.64	165.38	33.96
UCPEA-13	3.5 wt% NaOH	−361.30	4.789×10^{-4}	5.551×10^{-3}	441.75	79.37	73.20

steel strips and their coating properties were evaluated as shown in Table 1. Surface dry time of coatings was found to be UCPEA-7 (25 min), UCPEA-9 (23 min), UCPEA-11 (22 min), and UCPEA-13 (20 min). The scratch hardness values initially increase up to UCPEA-11 and then decrease. Since all coatings passed 250 lb/inch impact test, therefore, good adhesion between coatings and substrate was obtained. It has been observed that UCPEA coatings possessed good flexibility (bend test (1/8 in). Scratch hardness of coatings has been found to increase up to 11% of loading of TDI. Gloss at 45°C was found to be 84–93.

3.3.1. Corrosion Test. The exposure of panels in 3.5 wt% HCl solution, 5 wt% NaCl solution, tap water, and 3.5 wt% NaOH is made for 288 h, 168 h, 240 h, and 2 h, respectively. The polarization curves in HCl solution for uncoated MS and coated with UCPEA including NPs are shown in Figure 4(a). It has been observed that there is significant decrease for both anodic and cathodic currents of sample UCPEA relative to uncoated MS. The anodic and cathodic currents rate decreases and can be described by decrease in active area of electrodes. The tabulated values of E_{corr}, I_{corr}, corrosion rate, and inhibition efficiency after 288 h of exposure in 3.5 wt% HCl solution are shown in Table 2. The results indicate decrease in corrosion current of UCEPA-7, UCEPA-9, UCEPA-11, and UCEPA-13 as compared to uncoated mild steel. E_{corr}, corrosion rate for uncoated mild steel was −483.06 mV, 27.65 mm/yr. The corrosion rate was controlled to lesser values (1.309×10^{-6} mm/yr) by coating it with UCPEA-7, UCPEA-9, UCPEA-11, and UCPEA-13. Moreover, an increase in polarization resistance was observed.

The potentiodynamic polarization for uncoated MS and UCPEA coated MS after 168 h, immersion in 5 wt% NaCl solution can be described in Figure 4(b). It has been evident

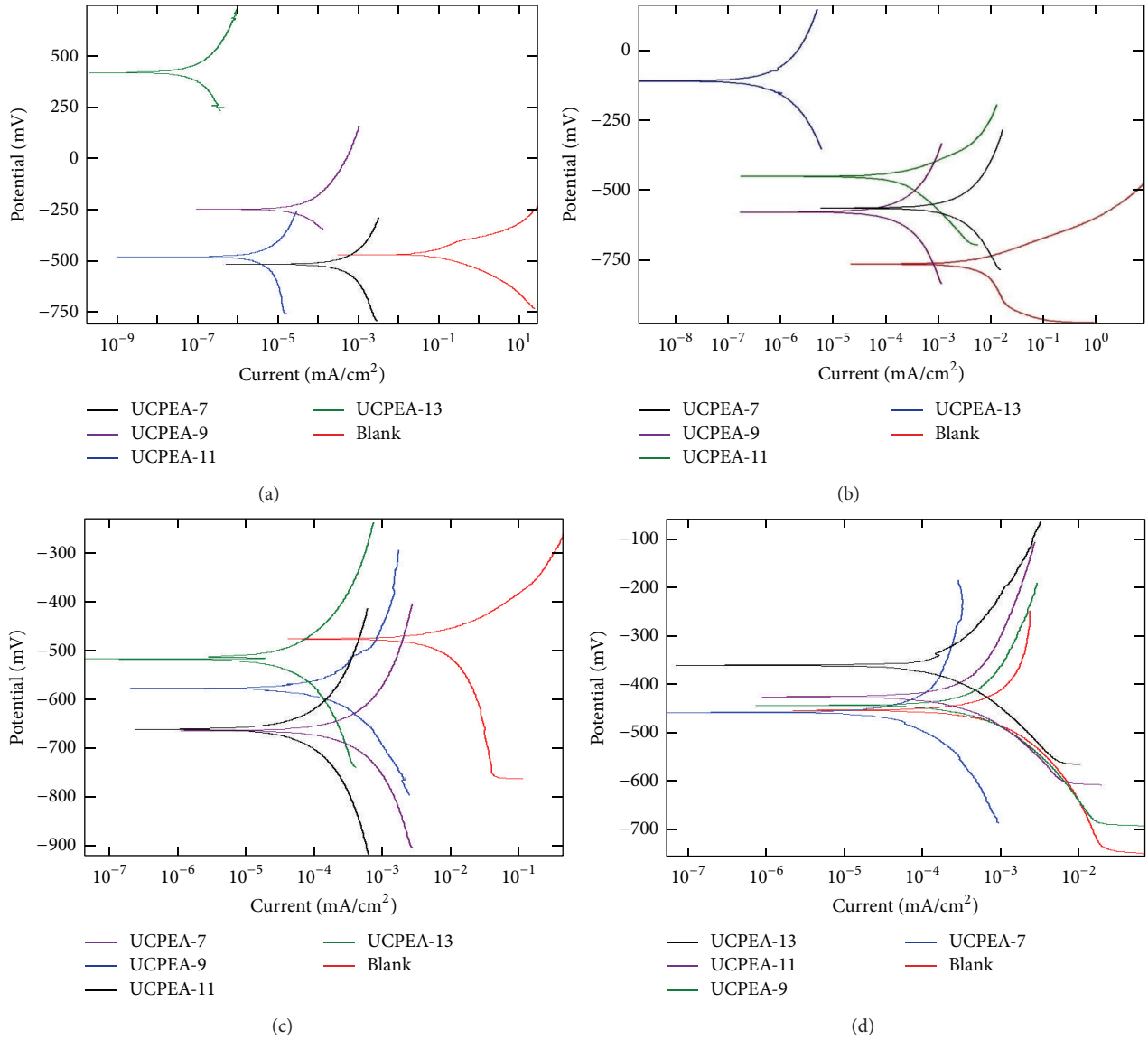

Figure 4: Tafel plots of coated with UCPEA in different media: (a) (3.5 wt% HCl), (b) (5 wt% NaCl), (c) (Tap water), and (d) (3.5 wt% NaOH) solution.

from the polarization curve that there was a remarkable potential shift to noble values for mild steel coated with UCPEA as compared to uncoated mild steel after immersed in 3.5 wt% HCl. The various polarization parameters such as E_{corr} and I_{corr} obtained from cathodic and anodic curves are shown in Table 2. This indicates that the E_{corr}, corrosion rate value for uncoated mild steel is −760.85 mV, 5.162 mm/yr. The corrosion rate can be controlled by coating mild steel with UCPEA-7, UCPEA-9, UCPEA-11, and UCPEA-13. The investigation clearly showed that UCPEA coated on mild steel controlled both anodic and cathodic reactions and UCPEA acted as barrier. In case of mild steel coated with UCPEA-7, UCPEA-9, UCPEA-11, and UCPEA-13, E_{corr} values (Table 2) were found to increase with increase in the amount of TDI in poly(urethane-esteramide).

The polarization curve recorded for uncoated MS and coated with UCPEA in tap water has been described in Figure 4(c). The cathodic and anodic polarization curves for the Tafel region were extrapolated and analyzed. E_{corr}, corrosion rate values for uncoated MS were found to be −474.96 mV, 3.901×10^{-1} mm/yr. Corrosion rate was controlled to lower values 1.113×10^{-4} mm/yr by coating it with UCPEA. The polarization curve recorded for uncoated MS and coated with UCPEA in 3.5% NaOH can be explained in Figure 4(d) and E_{corr} values (Table 2) indicate that UCPEA incorporated a good combination of ester, amide, urethane, and TiO_2 nanoparticles, which provided strong adhesion to the substrate. The coatings displayed good resistance against acid and saline environment. Commonly, it can be concluded that polyurethane developed from castor oil polyesteramide

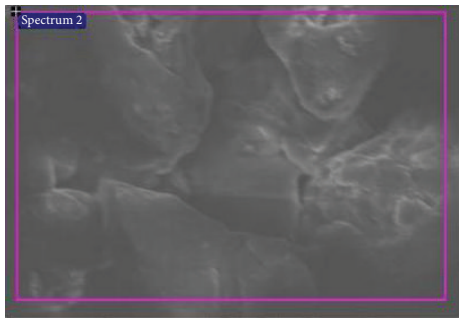

Figure 5: SEM of UCPEA13/TiO_2 nanocomposite.

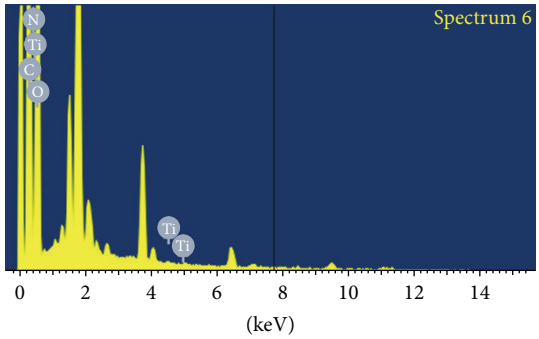

Full scale 1641 cts cursor: 7.700 (30 cts)

Figure 6: EDX of UCPEA13/TiO_2 nanocomposite.

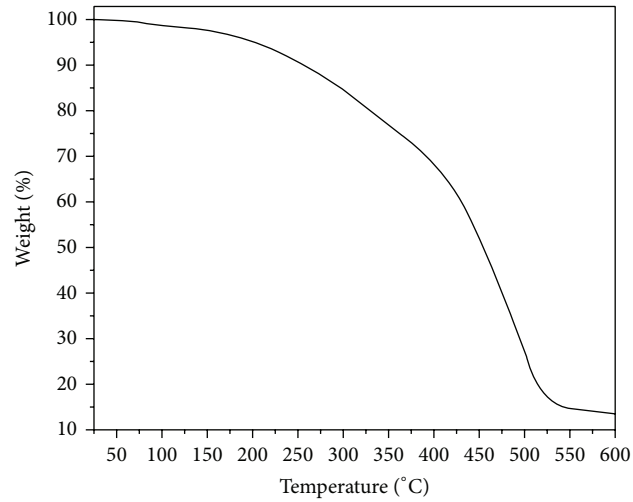

Figure 7: TGA thermogram of UCPEA-13/TiO_2 nanocomposite.

showed good resistance against acids and tap water. The physicomechanical performance revealed that UCPEA-13 showed best performance amongst all compositions in different corrosive media.

3.3.2. Scanning Electron Microscopy (SEM) and Energy-Dispersive X-Ray Spectroscopy (EDX). SEM micrograph (Figure 5) of UCPEA13/TiO_2 nanocomposite coating shows uniform coating without any visible cracks, which are not well-defined in shape and found to be well trapped in the polymer matrix. EDX results indicate the TiO_2 nanoparticles trapped in polymer matrix. Figure 6 shows UCPEA13/TiO_2 nanocomposite confirming that coating contains Ti and C, N, and O atoms. The peak observed at 0.3, 0.4, and 0.6 keV corresponds to binding energies of C, N, and O, respectively. These peaks observed at 0.4, 4.5, and 4.9 belong to Ti Lα, Ti Kα, and Ti Kβ. These optical absorption peaks are typical for absorption of metallic Ti nanocrystalline due to surface plasmon resonance.

3.4. Thermal Analysis. Thermogram of UCPEA-13 is shown in Figure 7. First degradation was started in range of 210 to 275°C and degradation resulted in 6% to 13% weight loss which was attributed to decomposition of urethane moieties. Another degradation between 275 and 500°C showed the major weight loss. This second degradation may be due to decomposition of amide groups, aromatic ring, aliphatic alkyl chain. In vegetable oil based polyurethanes, generally degradation starts after 150°C, due to the degradation of urethane moieties; however here the first step decomposition starts after 210°C. The relatively higher thermal stability can be correlated with the presence of TiO_2 NPs relative to virgin polyurethanes. 10 wt% loss was observed at 254°C and 50 wt% loss was observed at 450°C. The thermogram clearly shows that the nanocomposite can be safely used up to 200°C.

3.5. Antimicrobial Studies. Antimicrobial effect of UCPEA-13 against microbes was tested based on zone of inhibition. UCPEA-13 (0.4 wt% NPs in UCPEA-13) was subjected to antibacterial test against bacterial species, namely, *Staphylococcus aureus*, *Escherichia coli*, and *Bacillus pasteurii*, and fungal species, namely, *Fusarium solani*, *Penicillium notatum*, and *Aspergillus niger*. After 48 h of incubation at 27°C, inhibition zones of UCPEA-13 versus *Staphylococcus*, *Escherichia coli*, and *Bacillus pasteurii* were 14, 25, and 16 mm diameter, respectively. Moreover, the control did not show any zones of inhibition as shown in Figure 8. Antifungal effect of UCPEA-13 was checked against pathogenic fungi *Fusarium solani*, *Penicillium notatum*, and *Aspergillus niger*. The efficacy was determined after 72 h of incubation at 30°C. The inhibition zone diameters of UCPEA-13 against *Fusarium solani*, *Penicillium notatum*, and *Aspergillus niger* were found to be 26, 24, and 21 mm, respectively, as shown in Figure 9. UCPEA containing TiO_2 NPs exhibited good antimicrobial activity. TiO_2 NPs strongly bonded with electron donor groups in biological molecules containing oxygen, nitrogen, and sulphur. TiO_2 nanoparticles disturbed microorganism cell boundary and, as a result, rigid outermost cell layer lost its protection. Antimicrobial effect depends on size of nanoparticles to provide more dominant attack against microorganisms. TiO_2 NPs and their ions can produce free radicals resulting in induction of oxidative stress (i.e., reactive oxygen species; ROS). The produced ROS can permanently damage microbes and also cause microbes' death [30].

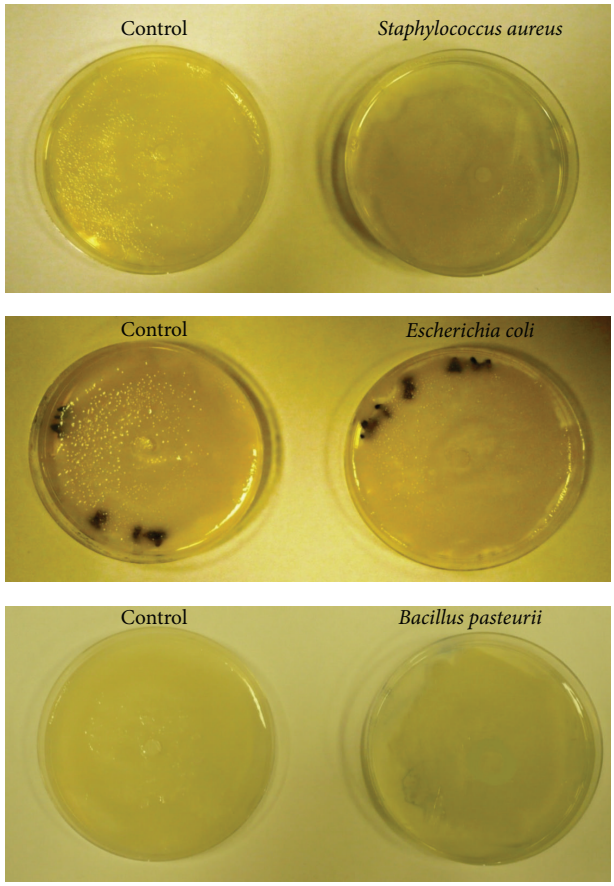

Figure 8: Antibacterial activity of UCPEA-13/TiO_2 nanocomposite.

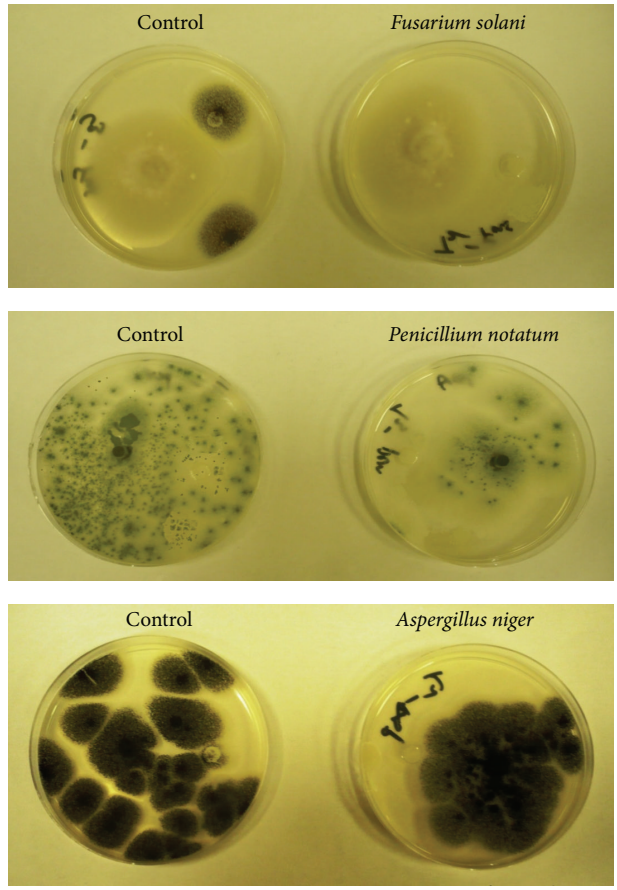

Figure 9: Antifungal activity of UCPEA-13/TiO_2 nanocomposite.

4. Conclusions

Poly(urethane-esteramide) nanocomposite coatings (UCPEA) were successfully synthesized and have been used as anticorrosive and antimicrobial and ecofriendly protective coating materials. The inclusion of minor amounts of TiO_2 NPs in the material leads to greater improvements in overall coating properties. The existence of nano-TiO_2 significantly improved scratch hardness, gloss, flexibility, pencil hardness, thermal stability, and microbial resistance of coatings, as compared to the virgin resins. UCPEA-13 showed the best physicomechanical and microbial and corrosion resistance among all UCPEA compositions. This coating can safely be used up to 200°C.

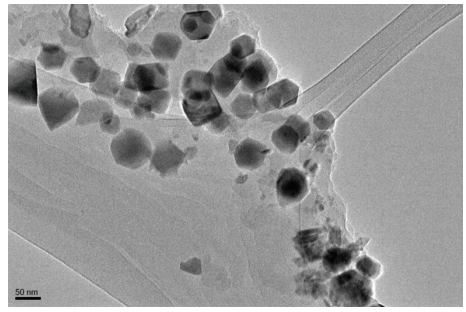

Figure 10: TEM image of TiO_2 nanoparticles.

Conflict of Interests

The authors declare that there is no conflict of interests.

Acknowledgment

The project was supported by Deanship of Scientific Research, Research Center, College of Science, King Saud University.

References

[1] A. I. Aigbodion, C. K. S. Pillai, I. O. Bakare, and L. E. Yahaya, "Synthesis, characterisation and evaluation of heated rubber seed oil and rubber seed oil-modified alkyd resins as binders in surface coatings," *Indian Journal of Chemical Technology*, vol. 8, no. 5, pp. 378–384, 2001.

[2] E. Can, S. Küsefoglu, and R. P. Wool, "Rigid thermosetting liquid molding resins from renewable resources. II. Copolymers of soybean oil monoglyceride maleates with neopentyl glycol and bisphenol A maleates," *Journal of Applied Polymer Science*, vol. 83, no. 5, pp. 972–980, 2002.

[3] S. Ramamurthi, V. Manohar, and V. V. S. Mani, "Characterization of fatty acid isomers in dehydrated castor oil by gas chromatography and gas chromatography-mass spectrometry techniques," *Journal of the American Oil Chemists' Society*, vol. 75, no. 10, pp. 1297–1303, 1998.

[4] P. L. Nayak, "Natural oil-based polymers: opportunities and challenges," *Journal of Macromolecular Science Part C: Polymer Reviews*, vol. 40, no. 1, pp. 1–21, 2000.

[5] M. Alam and N. M. Al-Andis, "Synthesis and characterization of poly(etherfattyamide) coatings from non edible seed oil," *Pigment and Resin Technology*, vol. 42, no. 3, pp. 195–201, 2013.

[6] F. Li, D. W. Marks, R. C. Larock, and J. U. Otaigbe, "Fish oil thermosetting polymers: synthesis, structure, properties and their relationships," *Polymer*, vol. 41, no. 22, pp. 7925–7939, 2000.

[7] R. V. Nimbalkar and V. D. Athawale, "Synthesis and characterization of canola oil alkyd resins based on novel acrylic monomer (ATBS)," *Journal of the American Oil Chemists' Society*, vol. 87, no. 8, pp. 947–954, 2010.

[8] S. Thakur and N. Karak, "Castor oil-based hyperbranched polyurethanes as advanced surface coating materials," *Progress in Organic Coatings*, vol. 76, no. 1, pp. 157–164, 2013.

[9] A. Chaudhari, V. Gite, S. Rajput, P. Mahulikar, and R. Kulkarni, "Development of eco-friendly polyurethane coatings based on neem oil polyetheramide," *Industrial Crops and Products*, vol. 50, pp. 550–556, 2013.

[10] E. Sharmin, S. M. Ashraf, and S. Ahmad, "Synthesis, characterization, antibacterial and corrosion protective properties of epoxies, epoxy-polyols and epoxy-polyurethane coatings from linseed and *Pongamia glabra* seed oils," *International Journal of Biological Macromolecules*, vol. 40, no. 5, pp. 407–422, 2007.

[11] S. Ahmad, S. M. Ashraf, E. Sharmin, F. Zafar, and A. Hasnat, "Studies on ambient cured polyurethane modified epoxy coatings synthesized from a sustainable resource," *Progress in Crystal Growth and Characterization of Materials*, vol. 45, no. 1-2, pp. 83–88, 2002.

[12] P. D. Meshram, R. G. Puri, A. L. Patil, and V. V. Gite, "Synthesis and characterization of modified cottonseed oil based Polyesteramide for coating applications," *Progress in Organic Coatings*, vol. 76, no. 9, pp. 1144–1150, 2013.

[13] M. Alam, D. Akram, E. Sharmin, F. Zafar, and S. Ahmad, "Vegetable oil based eco-friendly coating materials: a review article," *Arabian Journal of Chemistry*, vol. 7, no. 4, pp. 469–479, 2014.

[14] H. O. Sharma, M. Alam, U. Riaz, S. Ahmad, and S. M. Ashraf, "Miscibility studies of polyesteramides of linseed oil and dehydrated castor oil with poly(vinyl alcohol)," *International Journal of Polymeric Materials and Polymeric Biomaterials*, vol. 56, no. 4, pp. 437–451, 2007.

[15] R. D. Toker, N. Kayaman-Apohan, and M. V. Kahraman, "UV-curable nano-silver containing polyurethane based organic-inorganic hybrid coatings," *Progress in Organic Coatings*, vol. 76, no. 9, pp. 1243–1250, 2013.

[16] M. Behzadnasab, S. M. Mirabedini, K. Kabiri, and S. Jamali, "Corrosion performance of epoxy coatings containing silane treated ZrO_2 nanoparticles on mild steel in 3.5% NaCl solution," *Corrosion Science*, vol. 53, no. 1, pp. 89–98, 2011.

[17] A. Yabuki, W. Urushihara, J. Kinugasa, and K. Sugano, "Self-healing properties of TiO_2 particle-polymer composite coatings for protection of aluminum alloys against corrosion in seawater," *Materials and Corrosion*, vol. 62, no. 10, pp. 907–912, 2011.

[18] S. Dutta and N. Karak, "Synthesis, characterization of poly(urethane amide) resins from Nahar seed oil for surface coating applications," *Progress in Organic Coatings*, vol. 53, no. 2, pp. 147–152, 2005.

[19] M. Alam and N. Al-Aandis, "Synthesis and characterization of poly(styrene-co-maleic anhydride) modified pyridine polyesteramide coating from sustainable resource," *Pigment & Resin Technology*, vol. 41, no. 1, pp. 20–24, 2012.

[20] F. Zafar, E. Sharmin, S. M. Ashraf, and S. Ahmad, "Studies on poly (styrene-co-maleic anhydride)-modified polyesteramide -based anticorrosive coatings synthesized from a sustainable resource," *Journal of Applied Polymer Science*, vol. 92, no. 4, pp. 2538–2544, 2004.

[21] G. Knothe, S. C. Cermak, and R. L. Evangelista, "Methyl esters from vegetable oils with hydroxy fatty acids: comparison of lesquerella and castor methyl esters," *Fuel*, vol. 96, pp. 535–540, 2012.

[22] L. Guo, W. Yuan, Z. Lu, and C. M. Li, "Polymer/nanosilver composite coatings for antibacterial applications," *Colloids and Surfaces A: Physicochemical and Engineering Aspects*, vol. 439, pp. 69–83, 2013.

[23] A. Anand, R. D. Kulkarni, and V. V. Gite, "Preparation and properties of eco-friendly two pack PU coatings based on renewable source (sorbitol) and its property improvement by nano ZnO," *Progress in Organic Coatings*, vol. 74, no. 4, pp. 764–767, 2012.

[24] O. Eksik, A. T. Erciyes, and Y. Yagci, "*In situ* synthesis of oil based polymer composites containing silver nanoparticles," *Journal of Macromolecular Science, Part A: Pure and Applied Chemistry*, vol. 45, no. 9, pp. 698–704, 2008.

[25] S. K. Dhoke and A. S. Khanna, "Effect of nano-Fe_2O_3 particles on the corrosion behavior of alkyd based waterborne coatings," *Corrosion Science*, vol. 51, no. 1, pp. 6–20, 2009.

[26] S. Pramanik, K. Sagar, B. K. Konwar, and N. Karak, "Synthesis, characterization and properties of a castor oil modified biodegradable poly(ester amide) resin," *Progress in Organic Coatings*, vol. 75, no. 4, pp. 569–578, 2012.

[27] N. P. Bharathi, M. Alam, A. Tasleemjan, and A. A. Hashmi, "Bioactive organotin materials: synthesis, characterization and antimicrobial investigation," *Journal of Inorganic and Organometallic Polymers and Materials*, vol. 19, no. 2, pp. 187–195, 2009.

[28] S. Mahshid, M. Sasani Ghamsari, M. Askari, N. Afshar, and S. Lahuti, "Synthesis of TiO_2 nanoparticles by hydrolysis and peptization of titanium isopropoxide solution," *Semiconductor Physics, Quantum Electronics & Optoelectronics*, vol. 9, no. 2, pp. 65–68, 2006.

[29] M. Alam, M. R. Shaik, and N. M. Alandis, "Vegetable-oil-based hyperbranched polyester-styrene copolymer containing silver nanoparticle as antimicrobial and corrosion-resistant coating materials," *Journal of Chemistry*, vol. 2013, Article ID 962316, 11 pages, 2013.

[30] M. J. Hajipour, K. M. Fromm, A. Akbar Ashkarran et al., "Antibacterial properties of nanoparticles," *Trends in Biotechnology*, vol. 30, no. 10, pp. 499–511, 2012.